Construction and Building Materials 414 (2024) 135024

Contents lists available at ScienceDirect

Construction and Building Materials

journal homepage: www.elsevier.com/locate/conbuildmat

Quantification of the effects of material properties and support conditions on under tie pad behavior

Jaeik Lee *, Arthur de O. Lima, Marcus S. Dersch, J. Riley Edwards

Rail Transportation and Engineering Center – RailTEC, Department of Civil and Environmental Engineering – CEE, Grainger College of Engineering – GcoE, University of Illinois at Urbana-Champaign – UIUC, 205 N. Mathews Ave., Urbana, IL 61801, USA

ARTICLE INFO

Keywords:
Under tie pad (UTP)
Resilient material
Laboratory experimentation
Static bedding modulus

ABSTRACT

Recent trends in train operations have increased the loading demands on tracks for higher-speed passenger trains and heavy axle load (HAL) freight trains. These have led to accelerated degradation of track infrastructure components with higher maintenance costs, while also having less availability of track to conduct maintenance due to increased train frequencies. Under tie pads (UTPs), which are resilient materials attached under the crosstie, have been widely adopted since the 1990s as an effective method to mitigate track degradation. However, given that the performance of UTPs can be influenced by different characteristics, it is essential to understand the behavior of UTPs under various track and train operating conditions. In this study, the performance of commercial UTPs and generic elastomeric materials with different properties and characteristics were evaluated using four test support conditions that replicate the ballast interface behavior. The performance of the UTP was quantified and compared based on the results of static bedding modulus (C_{stat}), contact area, and maximum and average pressure. The result demonstrated significant variations in C_{stat} values under different support conditions, with an average of 314% for commercial UTPs and 712% for generic materials. Furthermore, the increased sample thickness of commercial UTP resulted in an average of 8% increase in contact area and simultaneous 10% and 6% decrease in maximum and average pressure for 0.04 in. (1 mm) thickness increase. The findings from this study can provide insight into how material characteristics with different support conditions influence the performance of UTPs, which can guide the selection of appropriate UTP types to achieve specific maintenance and life cycle objectives under various track and train operating conditions.

1. Introduction

1.1. Background

Under tie pads (i.e., internationally referred to as “under sleeper pads”) are elastic components that provide a conformal resilient layer beneath the crosstie. One of the initial applications of UTPs can be traced back to the mid-1970s on the Tokaido Shinkansen line [1], and they have since been investigated and adopted more widely, especially in Europe. This can be attributed to their known benefits such as mitigating track structure deterioration with increased maintenance intervals [2] which led to UTP implementation as a standard on the Austrian Railways (OBB) by 2009 [3]. Given the increasing demand for higher-speed rail operations and the heavy axle lad (HAL) freight railroad environment, the degradation of track infrastructure components can be accelerated, resulting in higher maintenance costs. As such, UTPs are emerging as a solution to increase ballast life cycle and preserve track geometry (Fig. 1) [4].

UTPs are typically composed of synthetic rubber or polyurethane elastomer and have a foam structure that contains encapsulated air voids [6,7]. UTP advantages have been quantified through prior research over the past twenty years as summarized by Myskowski et al. [2]. The contact area between the bottom of a concrete crosstie and the ballast (typically between 0.2% and 19% of total area) can increase by as much as 47% after the application of UTPs [7–13]. This increase in crosstie bearing area results in a decrease in the average contact stress by as much as 8–12% which can lead to a reduction in ballast degradation [14]. UTPs are also employed for the reduction of ground-borne noise and vibration [15]. Reductions between 4 and 14 dB have been reported by Loy et al. [15] for frequencies relevant to structure-borne noise (i.e., above 50 Hz). However, several studies demonstrated that UTPs can increase rail [16] and crosstie accelerations [6,10,16–18] by up to 88%

* Corresponding author.
E-mail address: jaeik2@illinois.edu (J. Lee).

https://doi.org/10.1016/j.conbuildmat.2024.135024
Received 4 August 2023; Received in revised form 19 December 2023; Accepted 12 January 2024
Available online 18 January 2024

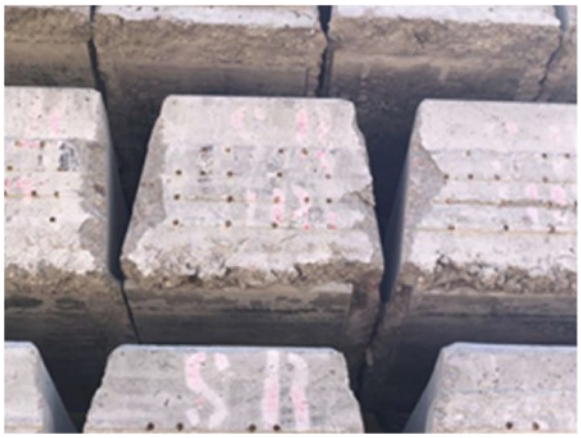

Fig. 1. Concrete crosstie with under tie pads (UTPs) [5].

and 150%, respectively.

Additionally, UTPs have recently been implemented and studied in a wide range of track locations and conditions including transition zones (e.g., open track to bridges) [19–21], rail joints [22], turnouts [23–25], and curves [5,26]. According to Wilk et al. [21], although the implementation of UTPs in the bridge approach section softens the approach instead of stiffening it, the reduction in ballast degradation and settlement is expected to exceed the negative effects arising from the increased stiffness differential between the bridge and approach section. Pen et al. [24] obtained field measurements in turnouts with two different characteristics of UTPs (i.e., soft and medium static bedding modulus) and found that the implementation of soft UTPs resulted in an approximate 40% increase in vertical crosstie movements compared to the turnout without UTPs, although the medium stiffness UTPs showed little difference. Wan et al. [25] developed a numerical model of a turnout and suggested optimized elasticity using various rail pad and UTP material properties. Although the results showed that the application of softer rail pads combined with UTPs can reduce dynamic forces in turnout frog section by up to 25%, Johansson et al. [6] demonstrated that the implementation of lower stiffness UTP can result in an increase in rail bending and displacement which is one of the primary concerns regarding the UTP implementation [27,28].

1.2. Approach

Although the implementation of UTPs generally improves the track performance and mitigates substructure degradation across different track conditions, it is crucial to determine the appropriate UTP properties considering their influence on track performance [29]. Therefore, the appropriate selection of UTP characteristics must consider the intent of their proposed application, such as noise and vibration mitigation, deflection adjustment, and settlement control. Among several parameters that reflect the expected performance and behavior of an UTP, the static bedding modulus (C_{stat}) was primarily investigated in this paper which is highly dependent on material type and thickness, and the applied load [30]. Gaining a deeper understanding of UTP performance as a function of these parameters can lead to improved UTP selection for different track conditions and applications. Branson et al. [31] demonstrated that thickness is one of the most influential parameters when selecting a UTP for contact pressure mitigation, but the study only considered a small number of materials under a single support condition. When determining C_{stat} per the European Standards (EN) 16730, the geometric ballast plate (GBP) is used to provide a representative ballast support condition and improve the repeatability of testing [32]. However, as demonstrated by Branson et al. [33], the GBP support condition overestimates the characteristics of contact compared to well-maintained ballast. Hence, the GBP cannot fully replicate the field crosstie-ballast contact condition and may lead to inaccurate estimation of field behavior. Kollmeier [34] conducted similar laboratory experiments under four different support conditions, including a GBP, albeit with a limited number of samples. Results showed considerable difference in C_{stat} depending on support conditions; values were highest for flat plate condition and lowest using the ballast-shaped plate developed by the Technical University of Munich (TUM), referred to as the TUM-plate.

With the results from prior research in mind, this paper evaluated the performance of both commercial UTPs and generic materials by quantifying the contact area, maximum and average pressures, and C_{stat} through laboratory experimentation. Different characteristics and material properties (e.g., thickness, hardness, and stiffness) were evaluated, and the results were compared across four different support conditions. Additionally, pressure and contact area result as a function of known sample properties will provide valuable insight into the selection of appropriate UTP properties for use in different track conditions.

2. Experimentation methods

2.1. Test setup configuration

Pre-determined loads were applied using a hydraulic actuator with a flat steel plate for even load distribution (Fig. 2). Samples were placed on each support condition followed by the sandpaper to simulate the concrete crosstie surface behavior. A 240- grit abrasive cloth was used based on the European Standards (EN) and American Railway Engineering and Maintenance-of-way Association (AREMA) recommendation to closely approximate the frictional characteristics of the concrete crosstie surface, aligning with the desired level of coarseness and roughness [32,35]. A matrix-based tactile surface sensor (MBTSS) was placed over the sandpaper to measure the pressure and contact area. These sensors consist of 44 printed electrically conductive rows and columns generating a total of 1936 sensing elements (i.e., sensels) providing a total active sensing area of 93.7 in^2 (605 cm^2) that allows for both qualitative and quantitative analysis of contact pressure distribution. Utilizing their raw output and known applied loads, maximum and average pressures are calculated, and contact area is determined as the sum of the area of all loaded sensels [31,36,37]. Lastly, three laser-based displacement sensors were deployed on three corners of the loading plate (defining a plane) to measure the specimen displacement.

2.2. Samples

In total, 25 different sample types were evaluated including 13 commercial UTP samples from four different manufacturers and 12 generic materials obtained from a stock material supplier. The component characteristics considered in the test matrix were hardness, thickness, and material type, with specific values provided in Tables 1 and 2. To address variability in test results three or more replicate samples were tested for each sample type, resulting in a total of 118 individual samples being tested.

2.3. Support conditions

Four different support conditions (i.e., flat plate, geometric ballast plate (GBP), ballast plate, and DIN plate) were used to simulate various possible crosstie-ballast contact behaviors (Fig. 3). Although the flat surface of the flat plate support is not representative of the contact interface for UTPs in revenue service, this procedure (i.e., compression test) is a well-known standard testing method to determine material behavior under a load and was employed to serve as a baseline reference. The GBP is included as a recommended support under EN standard testing procedures and consists of a steel plate with symmetrically arranged nodes designed to replicate the contact of ballast particles [32]. Its ease of implementation and repeatability among replicates are strong

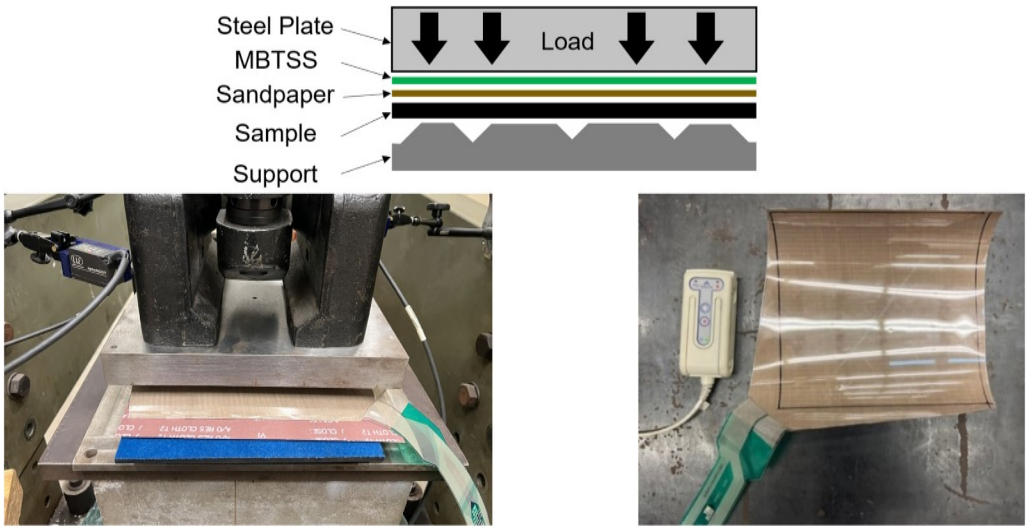

Fig. 2. Test setup configuration schematic (top), test setup with sample (bottom left), and detail of MBTSS (bottom right).

Table 1
Characteristics of commercial UTP materials included in laboratory testing matrix.

Manufacturer		Hardness (Shore A)	Thickness in. (mm)	Quantity (EA)	Size in. (mm)
Manufacturer A	A-1	68	0.28 (7)	5	9.843 × 9.843 (250 × 250)
	A-2	61	0.28 (7)	5	
	A-3	57	0.39 (10)	5	
	A-4	71	0.39 (10)	5	
	A-5	83	0.30 (7.5)	5	
Manufacturer B	B-1	68	0.22 (5.5)	5	
	B-2	63	0.28 (7)	5	
	B-3	67	0.28 (7)	5	
	B-4	69	0.39 (10)	5	
Manufacturer C	C-1	54	0.20 (5)	4	
	C-2	53	0.28 (7)	6	
	C-3	37	0.39 (10)	3	
	C-4	53	0.39 (10)	4	
Manufacturer D	D-1-A	42	0.20 (5)	5	
	D-1-B	58	0.32 (8)	5	
	D-2-A	46	0.20 (5)	5	
	D-2-B	53	0.32 (8)	5	

motivators for its use. The third support, the ballast plate, was cast using standard North American (N.A.) mainline ballast to simulate the interface with actual ballast while still providing repeatable support for all tests. Lastly, the Deutsches Institut fur Normung (DIN) plate is a legacy support plate used in the German DIN 45673 standard, the precursor to current the current EN UTP standard [32,38]. Similar to other supports, the DIN plate consists of a cast iron plate with a surface profile intended to replicate the ballast surface. Although DIN plate can reduce the variability of test results compared to actual ballast, the plate can still generate variability due to common geometric variations interinsic to its manufacturing and use (e.g., bending, curl, flatness, sample positioning, etc.).

Table 2
Characteristics of generic materials included in laboratory testing matrix.

Manufacturer		Hardness (Shore A)	Thickness in. (mm)	Quantity (EA)	Size in. (mm)
Generic material A (Neoprene rubber)	R-1	34	0.25 (6.35)	3	9.843 × 9.843 (250 × 250)
	R-2	50	0.25 (6.35)	3	
	R-3	40	0.37 (9.5)	3	
	R-4	54	0.37 (9.5)	3	
	R-5	42	0.50 (12.7)	3	
	R-6	59	0.50 (12.7)	3	
Generic material B (Polyurethane)	P-1	38	0.25 (6.35)	3	
	P-2	50	0.25 (6.35)	3	
	P-3	39	0.37 (9.5)	3	
	P-4	60	0.37 (9.5)	3	
	P-5	38	0.50 (12.7)	3	
	P-6	51	0.50 (12.7)	3	

2.4. Test procedure

Laboratory tests were conducted using AREMA recommended test procedures, which are based on EN standard procedures but account for N.A. railway operational differences [35]. The magnitude of applied loads were also obtained from AREMA (Table 3) and intended to represent the typical N.A. HAL freight load environment [35]. The freight loading condition had an associated p_{max} of 60 psi (413.7 kPa) which resulted in an applied load of 5.85 kips (26 kN) given the test sample's size.

Five cycles of quasi-static loading were applied to each sample within the range of 0.1 to 5.85 kips (0.44 to 26 kN) with a continuous loading and unloading rate of 1.45 psi/s (10 kPa/s). The first four preload cycles were applied to stabilize each sample and the load and displacement data from the final (fifth) cycle were used to calculate *Cstat*. To ensure uniform loading of the samples, displacements from each individual sensor should not differ by more than 20% from the

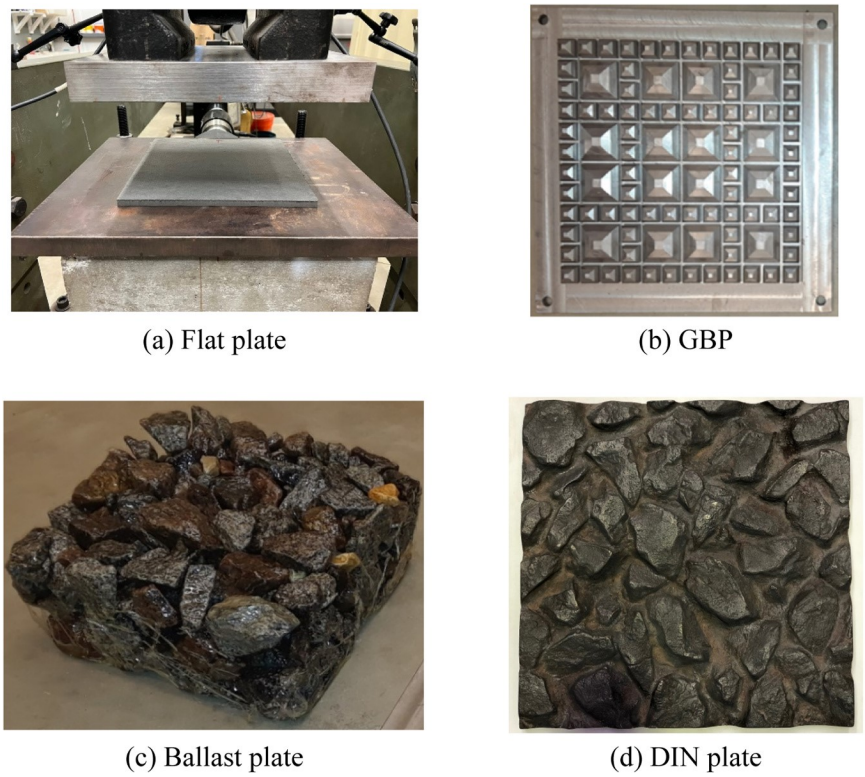

Fig. 3. Ballast support conditions used in laboratory testing.

Table 3
Pressures for static bedding modulus tests (adapted from AREMA, 2022).

Loading Environment	Typical Axle Load kips (kN)	p_{max} psi (kPa)	p_{min} psi (kPa)	Loading Rate psi/s (kPa/s)
Light Rail	21.8 (97.0)	22.0 (151.7)	1.45 (10.0)	1.45 ± 0.145 (10.0 ± 1)
Heavy Rail	25.6 (113.9)	29.0 (199.9)		
Commuter Rail	40.0 (177.9)	36.0 (248.2)		
Freight Rail	68.0 (302.5)	60.0 (413.7)		

average of all sensors. Values for *Cstat*, contact area, and maximum and average pressure were calculated and compared for each sample type under the different support conditions.

3. Laboratory experiment results

3.1. Effect of support condition on C_{stat}

Average C_{stat} results for commercial UTP types A through D and generic materials (i.e., rubber and polyurethane) under all four support conditions are shown in Fig. 4. Error bars are also included to represent the spread in the results for each sample type.

Results show that C_{stat} is on average 305%, 328%, and 276% higher under the flat plate support condition as compared to the GBP, ballast plate, and DIN plate, respectively. The variation of C_{stat} for commercial UTPs and generic materials under different support conditions ranged from 171% to 511% (average of 314%) and 431% to 990% (average of 712%), respectively. As observed, the *Cstat* of commercial UTP was significantly influenced by the support condition, especially in samples with a higher C_{stat}. Specifically, out of the total number of tested commercial UTP samples, the five samples with the highest C_{stat} values showed an average of 352% variation across four different support conditions, while the five samples with the lowest C_{stat} values showed an average variation of 241% depending on the different support condition. For the generic materials, the variation of C_{stat} values showed a 709% and 750% variation for the five samples with the highest C_{stat} values and five samples with the lowest C_{stat} values depending on the support conditions, respectively.

3.2. Effect of sample thickness and hardness on C_{stat}

To evaluate the effect of sample thickness and hardness, values for *Cstat* measured under GBP, ballast plate, and DIN plate support conditions were compared for all samples for which variation in these characteristics was available (i.e., UTP Type B, C, D-1, D-2, and rubber and polyurethane materials). The comparison across the samples were conducted considering the thickness increase of 0.04 in. (1 mm), and the results shown in Fig. 5 demonstrate that both thickness and hardness affect the magnitude of C_{stat}.

The decrease in C_{stat} values for commercial UTPs was on average of 0.033 kips/in^3 (0.009 N/mm^3), 0.023 kips/in^3 (0.006 N/mm^3), and 0.037 kips/in^3 (0.010 N/mm^3) under GBP, ballast plate, and DIN plate support conditions, respectively. The largest decrease among commercial UTPs was observed from UTP Type D with an average of 0.047 kips/in^3 (0.013 N/mm^3), followed by UTP Types B, and C with corresponding values of 0.032 kips/in^3 (0.009 N/mm^3), and 0.014 kips/in^3 (0.004 N/mm^3). While C_{stat} values generally decreased with increasing sample thickness, the magnitude of the reduction varied due to differences in material type. Exceptionally, the sample with a thickness of 0.28 in. (7 mm) exhibited a higher C_{stat} value than the 0.20 in. (5 mm) sample for Type C samples. This can be attributed to variability within the samples, particularly a higher sample thickness variation of up to 0.12 in. (3 mm) (i.e., unevenness) compared to other sample types, which have variations of less than 0.04 in. (1 mm).

Similarly, the generic materials showed decreases in average C_{stat} values by 0.023 kips/in^3 (0.006 N/mm^3), 0.024 kips/in^3 (0.006 N/mm^3), and 0.031 kips/in^3 (0.009 N/mm^3) under GBP, ballast plate, and

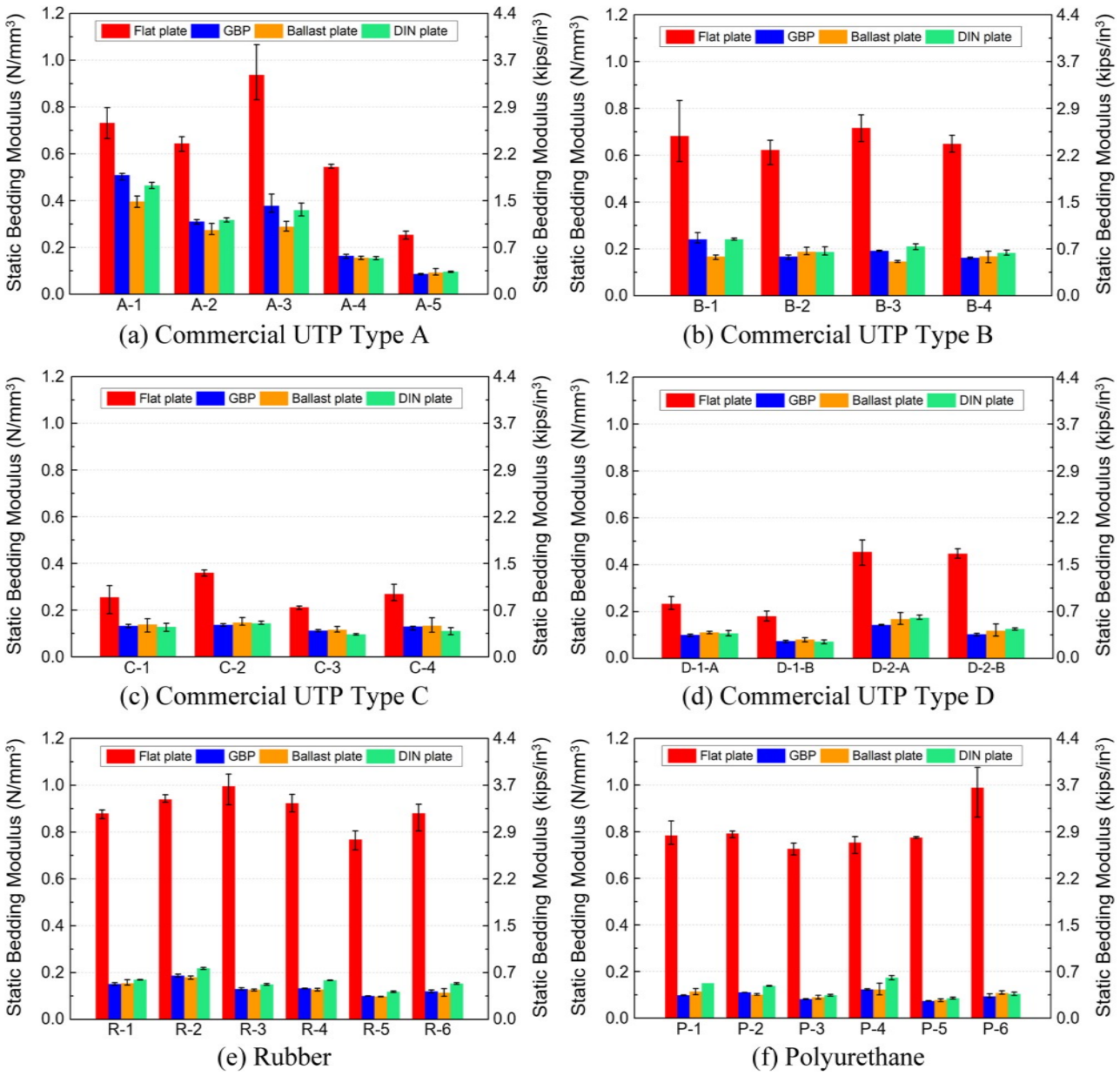

Fig. 4. C_{stat} results for commercial UTPs (a-d) and generic materials (e-f) under different support conditions.

DIN plate support conditions, respectively. However, the polyurethane 60 A samples with a thickness of 0.37 in. (9.5 mm) showed higher C_{stat} values compared to samples with a thickness of 0.25 in. (6.35 mm) and 0.50 in. (12.7 mm) across all support conditions. This difference can be attributed to the fact that the 0.37 in. (9.5 mm) samples were 10 Shore A higher in hardness compared to the other samples.

Further, the investigation into the effect of hardness was limited to generic materials, as commercial UTP samples within the test matrix were not available in different hardness. Results show that an increase of 20 Shore A hardness (i.e., 40 A to 60 A) resulted in 14%, 10%, and 13% increases in average C_{stat}, while an increase in sample thickness of 0.25 in. (6.35 mm) resulted in a decrease in average C_{stat} values by 30%, 28%, and 33% under GBP, ballast plate, and DIN plate support conditions, respectively. Overall, changes in thickness had a greater influence on C_{stat} than changes in surface hardness which aligns with earlier results presented by Branson et al. [31].

3.3. Effect of sample thickness on contact area and pressure

To evaluate the effect of sample thickness on pressure and contact area between the sample and support, values for contact area, maximum, and average pressures were measured and compared for both commercial UTPs and generic materials. The comparison across the samples was conducted considering the thickness increase of 0.04 in. (1 mm), and the results are presented below in Figs. 6 and 7, with numeric results shown in Tables 4 and 5.

for commercial UTPs and generic materials under ballast plate support condition (bottom).

Both commercial UTPs and generic materials showed decreased maximum pressure with an increase in sample thickness. The decrease in maximum pressure was more pronounced in commercial UTPs with an average decrease of 44.6 psi (0.31 MPa) compared to 24.0 psi (0.17 MPa) for generic materials. Among the commercial UTP samples, UTP Type D showed the highest ratio of decrease in maximum pressure, followed by Type B, Type A, and Type C. The corresponding maximum pressure decrease for these UTP types were 61.3 psi (0.42 MPa), 48.1 psi

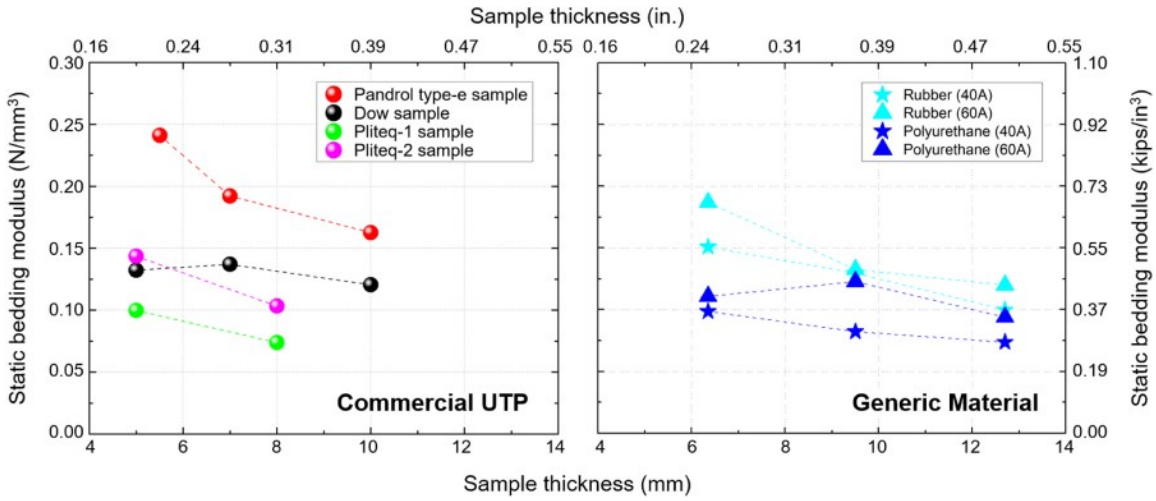

(a) GBP support condition

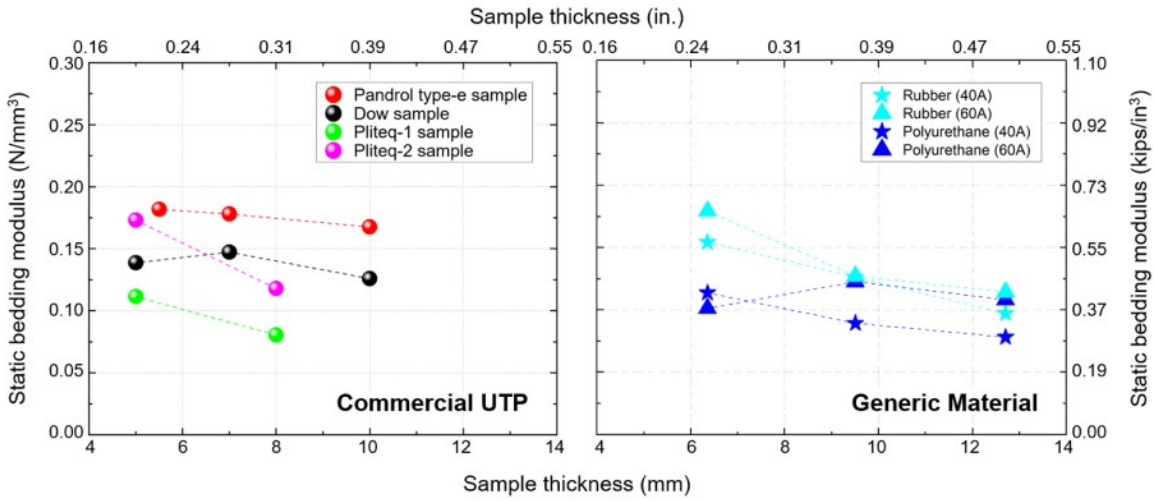

(b) Ballast plate support condition

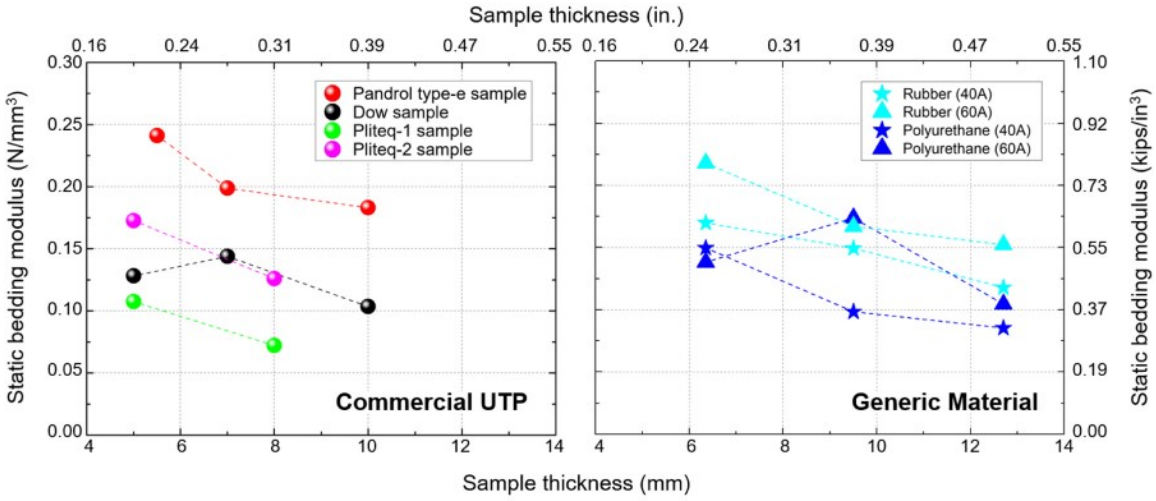

(c) DIN plate support condition

Fig. 5. Sample thickness and hardness effect on C_{stat} results under different support conditions.

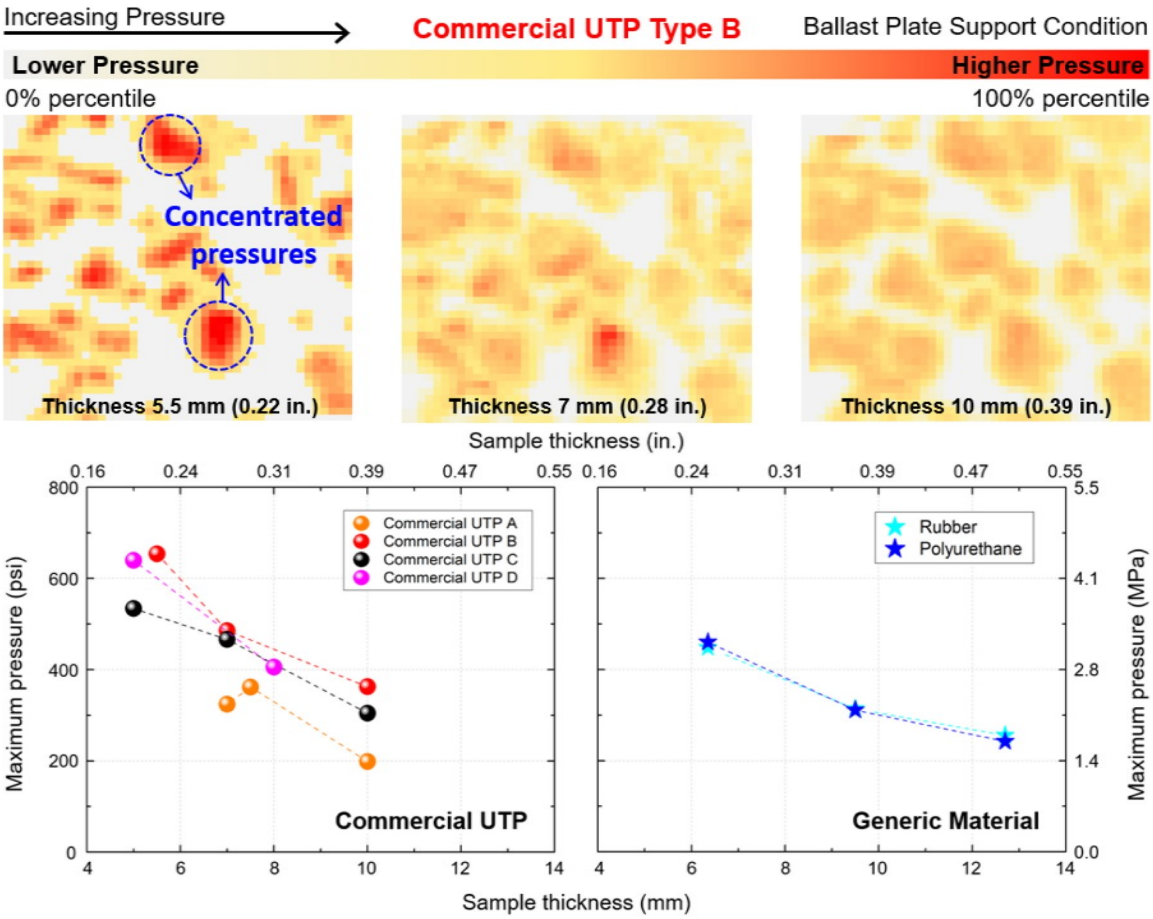

Fig. 6. MBTSS example results (top) and maximum pressure results.

(0.33 MPa), 36.9 psi (0.25 MPa), and 32.0 psi (0.22 MPa), respectively. Although Type A showed an increased pressure of 37.4 psi (0.26 MPa) with a thickness increase from 0.28 in. (7 mm) to 0.30 in. (7.5 mm), this is because the samples with a thickness of 0.30 in. (7.5 mm) have 19 Shore A higher hardness compared to samples with a thickness of 0.28 in. (7 mm). For the generic material, the maximum pressure for rubber and polyurethane decreased by 22.5 psi (0.16 MPa) and 25.6 psi (0.18 MPa), respectively. The highest pressures were observed under the ballast plate support condition, ranging from 186.0 to 725.7 psi (1.28 to 5.00 MPa) with an average of 443.2 psi (3.06 MPa) for commercial UTPs, and from 242.4 to 460.2 psi (1.67 to 3.17 MPa) with an average of 338.7 psi (2.34 MPa) for generic material. The maximum pressure under ballast plate was on average 49% and 32% higher compared to GBP support condition, and 37% and 15% for DIN plate support condition for commercial UTP and generic material, respectively. These findings indicate that the maximum pressure is more influenced by the support condition for commercial UTPs than for generic materials.

Both commercial UTPs and generic materials showed increased contact area with an increase in sample thickness. The increase in contact area was 5% higher in commercial UTPs with an average increase of 4.2 in^2 (27.1 cm^2) versus 4.0 in^2 (25.8 cm^2) for generic materials. Among the commercial UTP samples, UTP Type D showed the highest increase in contact area, followed by Type B, Type C, and Type A. The corresponding contact area increase ratio for these UTP types were 6.7 in^2 (42.9 cm^2), 5.7 in^2 (36.5 cm^2), 2.9 in^2 (18.5 cm^2), and 1.7 in^2 (11.2 cm^2), respectively. For the generic material, the contact area for rubber and polyurethane increased by 3.9 in^2 (25.2 cm^2) and 4.2 in^2 (27.1 cm^2), respectively. The highest contact area was observed under the GBP support condition, ranging from 51.0 in^2 (329.0 cm^2) to 92.7 in^2 (598.1 cm^2) with an average of 79.4 in^2 (512.0 cm^2) for commercial UTPs, and from 64.2 in^2 (414.2 cm^2) to 88.6 in^2 (571.6 cm^2) with an average of 77.3 in^2 (498.7 cm^2) for generic materials. The contact area under GBP support condition was on average 21% and 14% higher compared to ballast plate support condition, and 17% and 15% for DIN plate support condition for commercial UTPs and generic materials, respectively.

Additionally, given average pressures are calculated as the ratio of the applied load to the total contact area measured by the MBTSS sensor, and considering a consistent sample dimension and a uniform value for applied load, changes in contact area will be inversely proportional to the changes in average pressure. Hence, average pressure decreased by the same ratios.

4. Discussion

Among the four different support conditions tested, the results for C_{stat} were highest under the flat plate support condition, followed by DIN plate, GBP, and ballast plate. The higher results observed under the flat plate support condition can be attributed to the uniform distribution of load across the flat plate, engaging the entire sample area and resulting in lower displacements and higher C_{stat} values. The variation of C_{stat} was more pronounced for generic materials compared to commercial UTPs with an average difference of 398%. Also, the commercial UTPs with higher C_{stat} showed higher variation under different support conditions, while generic material showed inversed results which emphasize the importance of ballast support condition for commercial UTP implementation, especially for the higher C_{stat} samples.

For both commercial UTPs and generic materials, increased sample thickness resulted in an increased contact area and decreased maximum and average pressure, which contributes to mitigating substructure

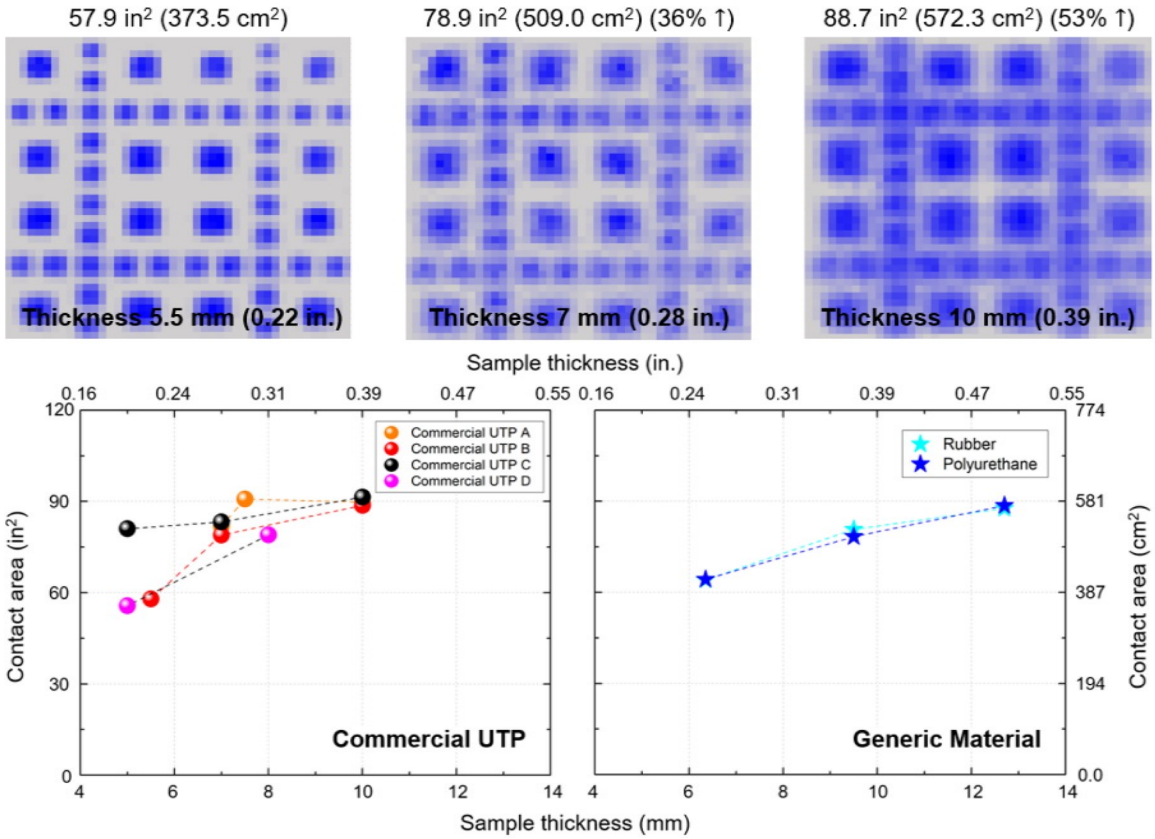

Fig. 7. MBTSS example (top) and contact area results for commercial UTPs and generic materials under GBP support condition (bottom).

Table 4
Maximum pressure results depending on sample thickness under different support conditions.

Material Type	Thickness Change, in. (mm)	GBP psi (MPa)		Ballast plate psi (MPa)		DIN plate psi (MPa)	
Commercial UTP Type A	0.28 to 0.39 (7 to 10)	229 to 145 (2.4 to 15.7)	37% ↓	362 to 198 (2.5 to 1.4)	45% ↓	260 to 161 (1.8 to 1.1)	38% ↓
Commercial UTP Type B	0.22 to 0.39 (5.5 to 10)	461 to 262 (3.2 to 1.8)	43% ↓	654 to 363 (4.5 to 2.5)	45% ↓	461 to 275 (3.2 to 1.9)	40% ↓
Commercial UTP Type C	0.20 to 0.39 (5 to 10)	288 to 192 (2.0 to 1.3)	33% ↓	534 to 305 (3.7 to 2.1)	43% ↓	381 to 226 (2.6 to 1.6)	41% ↓
Commercial UTP Type D	0.20 to 0.31 (5 to 8)	425 to 280 (2.9 to 1.9)	34% ↓	640 to 406 (4.4 to 2.8)	37% ↓	471 to 298 (3.2 to 2.1)	37% ↓
Generic material A (Neoprene Rubber)	0.25 to 0.5 (6.35 to 12.7)	295 to 184 (2.0 to 1.3)	37% ↓	449 to 256 (3.1 to 1.8)	43% ↓	349 to 225 (2.4 to 1.5)	36% ↓
Generic material B (Polyurethane)	0.25 to 0.5 (6.35 to 12.7)	284 to 176 (2.0 to 1.2)	39% ↓	460 to 242 (3.2 to 1.7)	47% ↓	383 to 222 (2.6 to 1.5)	42% ↓

Table 5
Contact area results depending on sample thickness under different support conditions.

Material Type	Thickness Change, in. (mm)	GBP in² (cm²)		Ballast plate in² (cm²)		DIN plate in² (cm²)	
Commercial UTP Type A	0.28 to 0.39 (7 to 10)	81.9 to 90.8 (529 to 586)	11% ↑	69.4 to 78.6 (448 to 507)	13% ↑	73.3 to 80.6 (473 to 520)	10% ↑
Commercial UTP Type B	0.22 to 0.39 (5.5 to 10)	57.9 to 88.7 (374 to 572)	53% ↑	46.2 to 72.2 (298 to 466)	56% ↑	50.9 to 74.5 (328 to 481)	47% ↑
Commercial UTP Type C	0.20 to 0.39 (5 to 10)	81.0 to 91.4 (523 to 590)	13% ↑	63.3 to 81.8 (408 to 527)	29% ↑	66.1 to 79.7 (426 to 514)	21% ↑
Commercial UTP Type D	0.20 to 0.31 (5 to 8)	55.7 to 79.0 (359 to 510)	42% ↑	46.2 to 65.9 (298 to 425)	43% ↑	49.9 to 66.8 (322 to 431)	34% ↑
Generic material A (Neoprene Rubber)	0.25 to 0.5 (6.35 to 12.7)	64.2 to 87.7 (414 to 565)	37% ↑	50.3 to 77.6 (324 to 501)	54% ↑	52.8 to 77.2 (341 to 498)	46% ↑
Generic material B (Polyurethane)	0.25 to 0.5 (6.35 to 12.7)	64.3 to 88.6 (415 to 572)	38% ↑	53.1 to 81.7 (342 to 527)	54% ↑	52.3 to 78.6 (337 to 507)	50% ↑

degradation. However, it can also lead to higher manufacturing costs and a decrease in the C_{stat} which may lead to increased track deflection and reduction in track stiffness. Additionally, the effect of different support conditions was investigated, and the lowest values for maximum and average pressure were observed under the GBP support condition, while the highest values were observed under the ballast plate support condition. For the contact area, the highest values were observed under GBP support condition while the lowest values were observed under ballast plate support condition which demonstrates the importance of appropriate selection of support condition to replicate the ballast interface.

5. Conclusions

This paper presented results from laboratory experiments for the quantification of UTP behavior with different properties and characteristics (i.e., thickness, stiffness, material) under four different support conditions. Based on the analysis and comparison of a total of 472 tests in 118 different samples the following conclusions are presented:

- Tested samples resulted in a high variation of C_{stat} values under different support conditions, with an average of 314% for commercial UTPs and 712% for generic materials. Materials with high variation in C_{stat} are not ideal for field implementation since they can result in variations in track deflection for adjacent track sections depending on ballast support condition.
- Among all tested commercial UTP samples, the five samples with the highest C_{stat} values showed an average 352% variation across four different support conditions, while the five samples with the lowest C_{stat} values showed an average variation of 241%, which highlights the significant impact of the ballast support condition on the commercial UTPs with higher C_{stat}.
- Although the increased sample thickness of commercial UTP resulted in improved performance with an average of 8% increase in contact area and simultaneous 10% and 6% decrease in maximum and average pressure for 0.04 in. (1 mm) thickness increase, it is crucial to carefully consider and negotiate the appropriate properties of UTP for different objectives under different track and train operating conditions.

The above conclusions provide an estimate of the response and behavior of the UTP with the changes in material properties (i.e., thickness, stiffness, etc.) under four different support conditions (i.e., flat plate, GBP, ballast plate, and DIN plate). Results provide insights for guiding the design and selection of appropriate UTP properties and characteristics to improve track performance under various track and train operating conditions. Additionally, the results obtained from laboratory experimentation can serve as preliminary information for the development of advanced and standardized guidelines, aiming to determine the suitable properties of UTPs. Nevertheless, it should be noted that the laboratory experiments only considered samples within specific conditions and results may not translate to other materials. Further testing is recommended to investigate samples with other material conditions as they might present different behavior under various support conditions.

CRediT authorship contribution statement

Lee Jaeik: Writing – original draft, Visualization, Formal analysis, Data curation. **de Oliveira Lima Arthur:** Writing – review & editing, Project administration, Methodology, Funding acquisition, Data curation, Conceptualization. **Edwards J. Riley:** Writing – review & editing, Supervision, Project administration, Funding acquisition, Conceptualization. **Dersch Marcus S.:** Supervision, Project administration, Methodology, Conceptualization.

Declaration of Competing Interest

The authors declare that they have no known competing financial interests or personal relationships that could have appeared to influence the work reported in this paper.

Data availability

The data that has been used is confidential.

Acknowledgements

This research was primarily supported by the BNSF Railway, with provision of products from the UTP supplier community. Authors would also like to thank Ehyeok Choi and Joohee Yim for their assistance with laboratory experimentation.

References

[1] Y. Katoh, H. Kakegawa, 1977. Effects of Rubber-pad under Concrete Tie on Pulverization of Ballast, Vibration and Noise, Quarterly Report of RTRI. 18, 10–14.
[2] B. Myskowski, A. de Oliveira Lima, J.R. Edwards, Under tie pads in railways - a state of the art review, Constr. Build. Mater. 383 (2022), https://doi.org/10.1016/j.conbuildmat.2023.131239.
[3] F. Auer, R. Schilder, Technical and economical aspects to under sleeper pads – part 1: long-term experiences in the obb-network, ZEVrail 133 (2009) 180–193.
[4] S.K. Navaratnarajah, B. Indraratna, Use of rubber mats to improve the deformation and degradation behavior of rail ballast under cyclic loading, J. Geotech. Geoenviron. Eng. 143 (6) (2017), https://doi.org/10.1061/(ASCE)GT.1943-5606.0001669.
[5] S. Kaewunruen, A.M. Remennikov, Under sleeper pads: field investigation of their role in detrimental impact mitigation, in: Proceedings of the 13th International Railway Engineering Conference, Edinburgh, Scotland, 2015: pp. 1–17.
[6] A. Johansson, J.C.O. Nielsen, R. Bolmsvik, A. Karlström, R. Lundén, Under sleeper pads—influence on dynamic train–track interaction, Wear 265 (2008) 1479–1487, https://doi.org/10.1016/j.wear.2008.02.032.
[7] C. Jayasuriya, B. Indraratna, T. Ngoc Ngo, Experimental study to examine the role of under sleeper pads for improved performance of ballast under cyclic loading, Transp. Geotech. 19 (2019) 61–73, https://doi.org/10.1016/j.trgeo.2019.01.005.
[8] T. Abadi, L. Le Pen, A. Zervos, W. Powrie, Measuring the area and number of ballast particle contacts at sleeper-ballast and ballast-subgrade interfaces, Int. J. Railw. Technol. 4 (2015) 45–72, https://doi.org/10.4203/ijrt.4.2.3.
[9] P.J. Gräbe, B.F. Mtshotana, M.M. Sebati, E.Q. Thünemann, The effects of under-sleeper pads on sleeper-ballast interaction, J. South Afr. Inst. Civ. Eng. 58 (2016) 35–41, https://doi.org/10.17159/2309-8775/2016/v58n2a4.
[10] Y. Guo, J. Wang, V. Markine, G. Jing, Ballast mechanical performance with and without under sleeper pads, KSCE J. Civ. Eng. 24 (2020) 3202–3217, https://doi.org/10.4203/ijrt.4.2.3.
[11] F. Pospischil, H. Loy, Sustainable superstructure with Under Sleeper Pads, Proceedings of 7th Transport Research Arena TRA 2018. 2018. https://www.researchgate.net/publication/329450238_Sustainable_superstructure_with_ Under_Sleeper_Pads.
[12] S. Potocan, T. Dorfner, Under sleeper pads for life cycle management used in building sustainable high quality tracks, in: 10th International Heavy Haul Association Conference, New Delhi, India, 2013: pp. 117–122.
[13] M. Sol-Sánchez, F. Moreno-Navarro, M.C. Rubio-Gámez, Viability of using end-of-life tire pads as under sleeper pads in railway, Constr. Build. Mater. 64 (2014) 150–156, https://doi.org/10.1016/j.conbuildmat.2014.04.013.
[14] S.K. Navaratnarajah, B. Indraratna, N.T. Ngo, Influence of under sleeper pads on ballast behavior under cyclic loading: experimental and numerical studies, J. Geotech. Geoenviron. Eng. 144 (2018) 1–16, https://doi.org/10.1061/(ASCE)GT.1943-5606.0001954.
[15] H. Loy, A. Augustin, L. Tschann, Reduction of vibration emissions and secondary airborne noise with under-sleeper pads—effectiveness and experiences, in: 12th International Workshop on Railway Noise, Terrigal, Australia, 2016: pp. 12–16.
[16] P. Schneider, R. Bolmsvik, J.C.O. Nielsen, In situ performance of a ballasted railway track with under sleeper pads, Proc. Inst. Mech. Eng. Part F J. Rail Rapid Transit. 225 (2011) 299–309, https://doi.org/10.1177/2041301710392479.
[17] P. Ferreira, R. Maciel, J. Estaire, M. Rodriguez-Plaza, Railway track design optimisation for enhanced performance at very high speeds: experimental measurements and computational estimations, Struct. Infrastruct. Eng. 15 (2019) 1–13, https://doi.org/10.1080/15732479.2018.1490325.
[18] N. Kumar, B. Suhr, S. Marschnig, P. Dietmaier, C. Marte, K. Six, Micro-mechanical investigation of railway ballast behavior under cyclic loading in a box test using DEM: effects of elastic layers and ballast types, Granul. Matter 21 (2019), https://doi.org/10.1007/s10035-019-0956-9.
[19] T. Dahlberg, On the use of under-sleeper pads in tracks with varying track stiffness, in: 9th International Heavy Haul Conference, Beijing, China, 2009: pp. 293–299.
[20] A. Paixão, C. Alves Ribeiro, N. Pinto, E. Fortunato, R. Calçada, On the use of under sleeper pads in transition zones at railway underpasses: experimental field testing,

Struct. Infrastruct. Eng. 11 (2015) 112–128, https://doi.org/10.1080/15732479.2013.850730.
[21] S.T. Wilk, T.D. Stark, W. Moorhead, Under-tie pads to improve track resiliency in railroad transition zones, in: Proc. 96th Annu. Meet. Transp. Res. Board Natl. Acad., Washington, DC, USA, 2017.
[22] S. Kaewunruen, A. Aikawa, A.M. Remennikov, Vibration attenuation at rail joints through under sleeper pads, Procedia Eng. 189 (2017) 193–198, https://doi.org/10.1016/j.proeng.2017.05.031.
[23] I. Grossoni, Y. Bezin, S. Neves, Optimisation of support stiffness at railway crossings, Veh. Syst. Dyn. 56 (2018) 1072–1096, https://doi.org/10.1080/00423114.2017.1404617.
[24] L. Le Pen, G. Watson, A. Hudson, W. Powrie, Behaviour of under sleeper pads at switches and crossings – field measurements, Proc. Inst. Mech. Eng. F J. Rail Rapid Transit. 232 (2018) 1049–1063, https://doi.org/10.1177/0954409717707400.
[25] C. Wan, V. Markine, I. Shevtsov, Optimisation of the elastic track properties of turnout crossings, Proc. Inst. Mech. Eng. F J. Rail Rapid Transit. 230 (2014) 360–373, https://doi.org/10.1177/0954409714542478.
[26] R. Müller, Y. Brechbühl, Measurement report about a new under sleeper test track in a curve, Report of International Union of Railways (UIC). 2013.
[27] W. Stahl, Improvement of ballasted tracks using sleeper pads - Investigations and experiences in Germany, in: Proceedings Seventh International Conference on the Bearing Capacity of Roads, Railways and Airfields, Trondheim, Norway, 2005.
[28] R. Insa, P. Salvador, J. Inarejos, L. Medina, Analysis of the performance of under-sleeper pads in high-speed line transition zones, Proc. Inst. Civ. Eng. Transp. 167 (2014) 63–77, https://doi.org/10.1680/tran.11.00033.
[29] A.L.O. de Melo, S. Kaewunruen, M. Papaelias, Parameters and boundary conditions in modelling the track deterioration in a railway system, IOP Conf. Ser. Mater. Sci. Eng. 603 (3) (2019) 032084, https://doi.org/10.1088/1757-899X/603/3/032084.
[30] C. Kraśkiewicz, A. Zbiciak, W. Oleksiewicz, W. Karwowski, Static and dynamic parameters of railway tracks retrofitted with under sleeper pads, Arch. Civ. Eng. LXIV (2018) 187–201, https://doi.org/10.2478/acc-2018-0070.
[31] J.M. Branson, M.S. Dersch, A. de O. Lima, J.R. Edwards, J. Cesar Bastos, Identification of the under-tie pad material characteristics for stress state reduction, Proc. Inst. Mech. Eng. F J. Rail Rapid Transit. 234 (2020) 1227–1237, https://doi.org/10.1177/0954409719890156.
[32] E CEN, Railway applications – Track – Concrete sleepers and bearers with under sleeper pads, European Committee for Standardization, Brussels, Belgium, 2016.
[33] J.M. Branson, M.S. Dersch, A. de Oliveira Lima, J.R. Edwards, J.Y. Kim, Analysis of geometric ballast plate for laboratory testing of resilient track components, Transp. Geotech. 20 (2019) 100240, https://doi.org/10.1016/j.trgeo.2019.04.003.
[34] V. Kollmeier, Development and use of tests on under tie pads in regards to the european standard, in: International Crosstie and Fastening System Symposium, Champaign, IL, USA, 2021.
[35] AREMA, Chapter 30: Ties, in: AREMA Manual for Railway Engineering, American Railway Engineering and Maintenance-of-way Association (AREMA), Landover, Maryland, United States, 2022.
[36] M.T. McHenry, M. Brown, J. LoPresti, J. Rose, R. Souleyrette, Use of matrix-based tactile surface sensors to assess fine-scale ballast–tie interface pressure distribution in railroad track, Transp. Res. Rec. J. Transp. Res. Board. 2476 (2015) 23–31, https://doi.org/10.3141/2476-04.
[37] C.T. Rapp, M.S. Dersch, J.R. Edwards, C.P.L. Barkan, B. Wilson, J. Mediavilla, Measuring rail seat pressure distribution in concrete crossties: experiments with matrix-based tactile surface sensors, Transp. Res. Rec. J. Transp. Res. Board. 2374 (2013) 190–200, https://doi.org/10.3141/2374-22.
[38] Deutsches Institut für Normung (DIN) 45673, Mechanical vibration – Resilient elements used in railway tracks, Berlin, Germany, 2010.